# Road Maps for Nitrogen-Transfer Catalysis: The Challenge of the Osmium(VIII)-Catalyzed Diamination

**Dirk V. Deubel*[a] and Kilian Muñiz[b]**

**Abstract:** Although the Sharpless dihydroxylation has been used on laboratory and industrial scales for several decades, an analogous osmium-catalyzed diamination is unknown. To explore the reaction of osmium(VIII) oxo–imido complexes with C=C bonds, density functional calculations have been performed. The calculations predict a chemoselective and perispecific [3+2] addition of the NH=Os=NH moiety of diimidodioxoosmium(VIII) to ethylene, yielding dioxoosma-2,5-diazolidine. At first sight, this metallacycle seems extremely stable; it is more stable than diimidoosma-2,5-dioxolane by 40 kcal mol$^{-1}$. However, a comparison of the thermodynamic reaction profiles for catalytic model cycles of dihydroxylation, aminohydroxylation, and diamination reveals that, contrary to common belief, the instability of the metal=N bond in the osmium(VIII) imido complex rather than the stability of the metal–N bond in the osmium(VI) intermediate causes most of the energy difference between the metallacycles. Substituents on the substrate have a small effect on the thermodynamic reaction profiles, whereas substituents on the imido ligands allow steric and electronic control of the reaction free enthalpies in the range of up to 25 kcal mol$^{-1}$. The results of this study help identify potential challenges in the development of the as-yet hypothetical title reaction and provide a modular concept for exploring novel catalytic routes.

**Keywords:** density functional calculations · diamination · dihydroxylation · osmium

## Introduction

Because vicinal diamines have been used as ligands in asymmetric catalysis[1] and in platinum anticancer drugs,[2] exploring efficient strategies for their synthesis is of current interest.[3] An elegant catalytic route to vicinal diols and amino alcohols consists of the addition of osmium tetraoxide and its monoimido derivatives to olefins, subsequent oxidation of the metallacyles, and hydrolytic release of the products.[4] Twenty-three years after the pioneering work on the enantioselective catalytic dihydroxylation[5] and seven years after the first report of a stereoselective catalytic aminohydroxylation,[6] the reactions are still under active development.[7] However, an analogous osmium(**VIII**)-catalyzed diamination has not yet been discovered. Early work opened up the synthesis of imido complexes and demonstrated their reactivity to olefins; however, liberating the diamine requires a stoichiometric reductive workup of the metallacycles.[8] We present herein a density functional theory (DFT) study to identify potential challenges in as-yet hypothetical processes for the osmium(**VIII**)-catalyzed 1,2-diamination. The DFT methods used herein were previously employed for evaluating mechanistic suggestions of organometallic intermediates in metal-mediated oxygen-transfer reactions, focusing on the initial step of dihydroxylation.[9–11]

The paper is organized as follows: first, the peri- and chemoselectivity in the addition of diimidodioxoosmium(**VIII**) to ethylene is predicted and rationalized. Second, the thermodynamic reaction profile for a model cycle of catalytic dihydroxylation is predicted and compared to an analogous model cycle for diamination. Third, an analysis of the electronic structure of key intermediates and a study of substituent effects aim to show the steric and electronic control of the reaction free enthalpies. Fourth, an analogous scenario is developed for state-of-the-art catalytic aminohydroxylation, to which a corresponding diamination process is compared. Analyses of the nature of metal–ligand bonding ac-

[a] Dr. D. V. Deubel
Department of Chemistry and Applied Biosciences
ETH Zürich
USI Campus
Via Giuseppe Buffi 13
6900 Lugano (Switzerland)
http://www.staff.uni-marburg.de/~deubel/
E-mail: metals-in-medicine@phys.chem.eth.ch

[b] Dr. K. Muñiz
Kekulé-Institut für Organische Chemie und Biochemie
Rheinische Friedrich-Wilhelms-Universität
53121 Bonn (Germany)
http://www.chemie.uni-bonn.de/oc/muniz/Muniz.html
E-mail: kmuniz@uni-bonn.de

Supporting information for this article is available on the WWW under http://www.chemeurj.org/ or from the author.

 **DOI: 10.1002/chem.200305467**  

company the calculations, thus exploiting both the predictive and rationalizing power of our quantum-chemical approach.

## Results and Discussion

**Addition of oxo–imido complexes across C=C bonds**: The mechanism of the initial step of *cis*-dihydroxylation, the addition of osmium tetraoxide across a C=C bond, had been controversial for several decades, until quantum-chemical calculations together with experimental kinetic isotope effects showed a concerted [3+2] addition to be preferred over a stepwise mechanism (Scheme 1).[12,13] While the reaction of (pentamethylcyclopentadienyl)(trioxo)rhenium(-VIII)[10,14] and [tris(3,5-dimethyl pyrazolyl)](borato)(trioxo)-rhenium(VIII)[15] with C=C bonds also follows a [3+2] mechanism, recent quantum-chemical[10] and experimental[16] investigations revealed that certain "spectator" ligands L in $LReO_3$ may invert the relative height of the [3+2] and [2+2] barriers. Little is known about the mechanism if a "reactive" oxo ligand itself in metal oxides, such as osmium tetraoxide, is replaced by an imido ligand. Since reactions of imido complexes with C=C bonds are particularly relevant to the addition of amino functionalities to olefins, there is a current call for further studies on the mechanism of these nitrogen-transfer events.[4e,17]

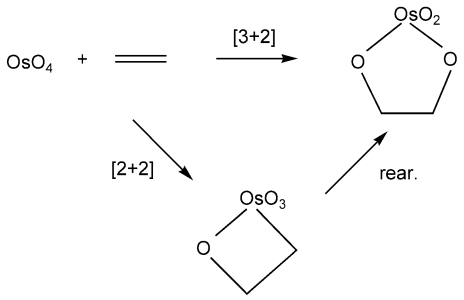


Scheme 1. [3+2] versus [2+2] addition of osmium tetraoxide to C=C bonds.

To clarify the mechanism of the reaction of osmium(VIII) oxo–imido complexes with olefins, density functional theory at the B3LYP level has been used. The reaction of diimidodioxoosmium(VIII) with ethylene has been studied, because precursors of vicinal diols, amino alcohols, and diamines could in principle be obtained (Scheme 2). Table 1 lists the theoretically predicted activation energies $\Delta E_a$ and activation free enthalpies $\Delta G_a$ (Gibbs free energies) for the addition of the Os=O, Os=NH, O=Os=O, O=Os=NH, and NH=Os=NH moieties to ethylene. Note that the $\Delta G_a$ values are systematically higher than the $\Delta E_a$ values by approximately 13 kcal mol$^{-1}$ (Table 1), arising primarily from the loss of translational and rotational entropy as a result of the bimolecular reaction. The calculations reveal the general trend that all activation free enthalpies for [2+2] additions (> 55 kcal mol$^{-1}$) are much higher than the activation free enthalpies $\Delta G_a$ for any [3+2] addition (<25 kcal mol$^{-1}$). Figure 1 displays the calculated transition structures for the [3+2] reactions. The predicted distances between the reactants in the TS (dashed lines) show that the TS for the NH=Os=NH addition is the earliest on the reaction coordinate and the TS for the O=Os=O addition is the latest, potentially indicating that the former reaction is fastest and the latter reaction is slowest.[18] Indeed, the activation free enthalpies for the [3+2] additions decrease in the order O=Os=O (23 kcal mol$^{-1}$) > O=Os=NH (20 kcal mol$^{-1}$) > NH=Os=NH (12 kcal mol$^{-1}$). These results are consistent with the products of the reaction of bis(*tert*-butylimido)(dioxo)osmium(-VIII) with olefins.[8] The calculated lengths of 1.72 Å for the Os−O double bond and of 1.92 Å for the Os−N single bond compare well to those observed in solid-state structures, namely 1.71–1.73 Å and 1.88–1.90 Å, respectively.[19]

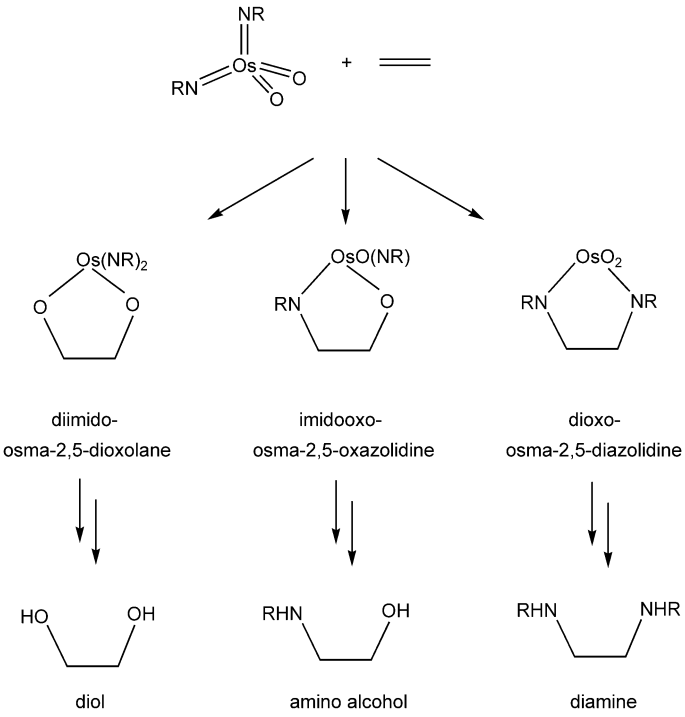


Scheme 2. Metallacycles as potential precursors of diols, amino alcohols, and diamines.

Table 1. Peri- and chemoselectivity in the addition of $OsO_2(NH)_2$ to ethylene. Activation energies ($\Delta E_a$) and reaction energies ($\Delta E_r$) calculated at the B3LYP/III+//B3LYP/II level and free enthalpies ($\Delta G_a$, $\Delta G_r$) at 298.15 K. All values in kcal mol$^{-1}$.

| Reaction | | $\Delta E_a$ | $\Delta G_a$ | $\Delta E_r$ | $\Delta G_r$ |
|---|---|---|---|---|---|
| [2+2] | Os=O[a] | 46.5 | 59.8 | 7.1 | 22.3 |
| [2+2] | Os=NH[a] | 42.5 | 56.3 | −8.4 | 8.5 |
| [3+2] | O=Os=O | 8.3 | 22.8 | −23.9 | −6.0 |
| [3+2] | O=Os=NH | 6.1 | 19.9 | −46.4 | −27.3 |
| [3+2] | NH=Os=NH | 0.4 | 12.1 | −67.2 | −46.2 |

[a] Only the stereoisomer lowest in energy is listed.

To rationalize the chemoselectivity of the reaction, a comparative energy decomposition analysis[20–23] of the $C_{2v}$-symmetric transition state for the O=Os=O addition shown in Figure 1 and of an analogous structure for the NH=Os=NH addition was performed. The analysis of the TS for the O=Os=O addition to ethylene is presented in Table 2. The

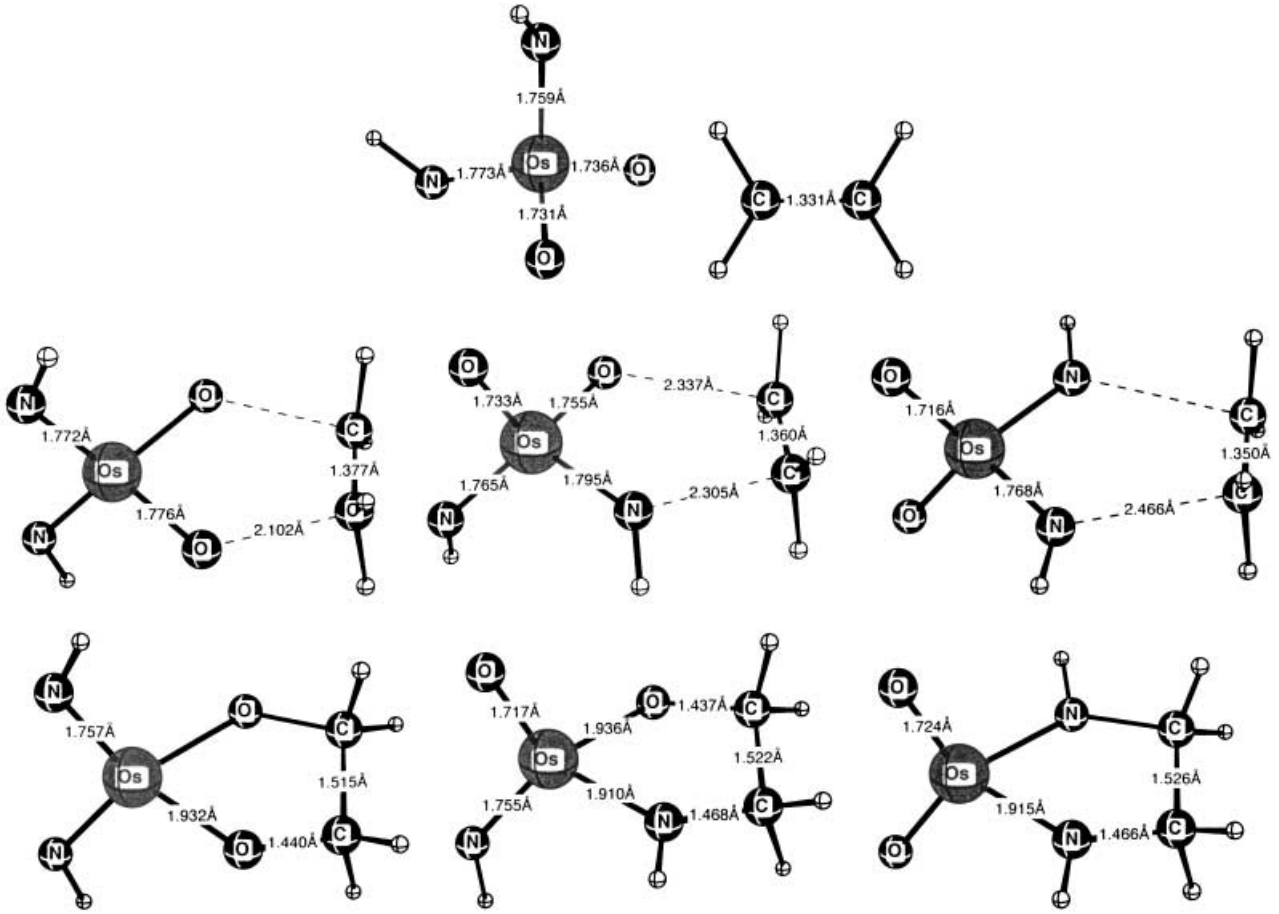


Figure 1. Calculated structures of the reactants (top), transition states (middle), and products (bottom) for the [3+2] additions of $OsO_2(NH)_2$ to ethylene.

Table 2. Factors governing the chemoselectivity in the addition of $OsO_2(NH)_2$ to ethylene. Energy decomposition of the $C_{2v}$-symmetric transition structures for the [3+2] addition of the O=Os=O and NH=Os=NH moieties calculated at the BLYP/IV′ level. Bold: Contributions from the $\Gamma_i$ symmetry orbitals to the stabilizing orbital-interaction energy $\Delta E_{orb}$. All energies in kcal mol$^{-1}$.

| Contribution | $\Gamma_i$ | O=Os=O | NH=Os=NH[a] | change in %[b] |
|---|---|---|---|---|
| $\Delta E_{str}$ ethylene | | 12.0 | 12.0 | |
| $\Delta E_{str}$ $OsO_2(NH)_2$ | | 15.2 | 10.0 | −34 |
| $\Delta E_{str}$ total | | 27.2 | 22.0 | |
| $\Delta E_{Pauli}$ | | 138.6 | 172.0 | 25 |
| $\Delta E_{elst}$ | | −65.8 | −81.8 | 24 |
| $\Delta E_{orb}$ | | −92.1 | −116.6 | 27 |
| **$\Delta E_{orb}$ ($\Gamma_i$)** | **$a_1$** | **−61.4** | **−70.6** | **15** |
| | **$a_2$** | **−1.3** | **−2.9** | |
| | **$b_1$** | **−1.2** | **−1.8** | |
| | **$b_2$** | **−28.2** | **−41.3** | **46** |
| $\Delta E_{int} = \Delta E_{Pauli} + \Delta E_{elst} + \Delta E_{orb}$ | | −19.4 | −26.4 | 36 |
| $\Delta E = \Delta E_{str} + \Delta E_{int}$ | | 7.8 | −4.4 | |
| $\Delta E_{orb}/\Delta E_{elst}$ | | 1.40 | 1.42 | |
| $\Delta E_{orb}(a_1)/\Delta E_{orb}(b_2)$ | | 2.17 | 1.71 | |

[a] To compare the two reactions, a post-TS structure for the NH=Os=NH addition was evaluated on the basis of a geometry with N–C distances set equal to the O–C distances in the TS for the O=Os=O addition (1.938 Å at BLYP/IV′) and with the Os–N distances set equal to the Os–O distance in the TS for the O=Os=O addition (1.809 Å at BLYP/IV′). [b] NH=Os=NH[a] relative to the O=Os=O TS.

method was previously described[21] and is implemented as follows: 1) the two reactants, metal complex and olefin, must be deformed from their equilibrium structure to their geometry in the transition states. This requires a strain energy $\Delta E_{str}$ = 12 and 15 kcal mol$^{-1}$ for ethylene and for the metal complex, respectively (Table 2). 2) The deformed reactants interact with each other. The interaction energy $\Delta E_{int}$ can be partitioned into three contributions: repulsion $\Delta E_{Pauli}$ of the two reactants on account of the Pauli principle, electrostatic interactions $\Delta E_{elst}$, and stabilizing orbital interactions $\Delta E_{orb}$. The sum of strain energy and interaction energy gives the activation energy $\Delta E$. The ratio $\Delta E_{orb}/\Delta E_{elst}$ of 1.4 indicates that stabilizing orbital interactions are more important than electrostatics in the TS and thus the reaction is orbital-controlled. In contrast, [2+2] additions of rhenium(VII) oxides to the C=C bond of ketene were shown to be charge-controlled, whereas organic [2+2] additions were shown to be orbital-controlled.[24]

The stabilizing orbital interactions can in turn be decomposed into the contributions from symmetry orbitals (Table 2). The $a_1$ and $b_2$ irreducible representations are

  

found to contribute significantly to $\Delta E_{orb}$, where $a_1$ corresponds to the electron donation from the π orbital of ethylene into a π* orbital of the metal complex (Figure 2, top),

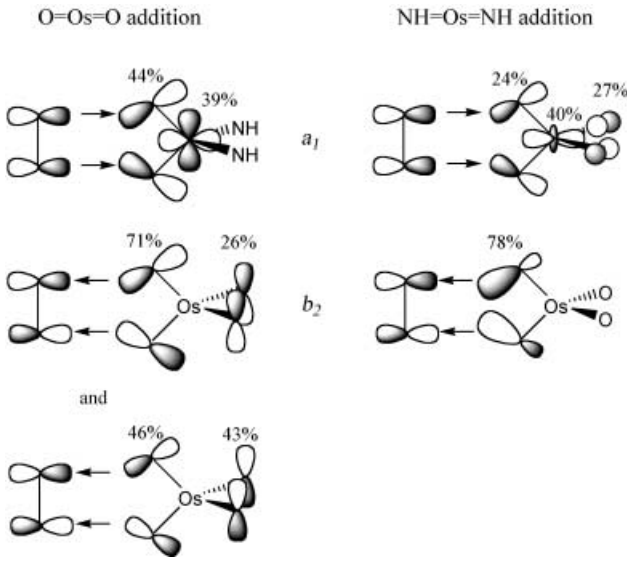


Figure 2. $a_1$ and $b_2$ symmetry orbitals in the $C_{2v}$-symmetric transition state for [3+2] additions of $OsO_2(NH)_2$ to ethylene. Orbital coefficients in $OsO_2(NH)_2$.

and $b_2$ corresponds to electron backdonation from the antisymmetric linear combinations of oxo lone pairs into the π* orbital of ethylene (Figure 2, bottom). The calculations reveal that the contribution of donation ($a_1$, 61 kcal mol$^{-1}$) to the stabilizing orbital-interaction energy is twice as high as that of backdonation ($b_2$, 28 kcal mol$^{-1}$).

The analysis of the TS for the NH=Os=NH addition to ethylene is also presented in Table 2. The theoretically predicted N−C distances of 2.47 Å show this transition state to be much earlier than the TS for the O=Os=O addition with O−C distances of 2.10 Å (at B3LYP, Figure 1). When analyzing the two reactions, it is important to know that the energy contributions are highly distance-dependent.[22,25] Therefore, a post-transition structure for the NH=Os=NH addition with N−C distances set equal to the O−C distances in the TS for the O=Os=O addition has been analyzed. The calculations show a much smaller strain energy $\Delta E_{str}$ in the structure for the NH=Os=NH addition (Table 2), indicating that the elongation of the Os=N bonds requires significantly less energy than the elongation of the Os=O bonds. Furthermore, in the structure for the NH=Os=NH addition, the contributions to the interaction energy have increased by approximately 25% compared to the TS for O=Os=O addition (Table 2). This is not surprising because the structure evaluated for the NH=Os=NH addition has already passed the transition state. The ratio of stabilizing orbital interactions and electrostatics is the same in both structures ($\Delta E_{orb}/\Delta E_{elst} = 1.4$). However, electron backdonation ($b_2$) from the antisymmetric linear combination of the imido lone pairs into the π* orbital of ethylene is larger than electron backdonation in the TS for the O=Os=O addition by approximately 45%. The larger atomic orbital coefficients on the N atoms in the occupied $b_2$ molecular orbital of $OsO_2(NH)_2$ in the NH=Os=NH addition (Figure 2) compared with those on the O atoms in the corresponding orbitals of the O=Os=O addition are in agreement with the relative strength of backdonation in the former reaction. This type of interaction is apparently an important factor which contributes to the chemoselectivity of the reaction.

The calculated reaction free enthalpies of the metalla-analogous cycloadditions are also presented in Table 1. In contrast to the addition of rhenium(VII) oxides across C=C bonds,[9,10] each activation free enthalpy reported in this work is in agreement with the thermodynamics of the reaction.[18] The [2+2] additions are predicted to be endergonic, while the [3+2] additions are exergonic (Table 1). Most remarkably, the calculations reveal a very large stability of the dioxoosma-2,5-diazolidine. This structure is more stable than the isomeric diimidoosma-2,5-dioxolane by 40 kcal mol$^{-1}$. The relative energy of imidooxoosma-2,5-oxazolidine, the potential precursor of an amino alcohol, lies in between, that is, it is more stable than the dioxolane by −21 kcal mol$^{-1}$. These very large energy differences of the five-membered metallacycles are not evident from their geometries, which do not show characteristic discrepancies (Figure 1).

One may anticipate that there is a price to be paid for the large energy gain in the initial step of diamination: ≈ 40 kcal mol$^{-1}$ relative to the formation of the oxygen-containing metallacyle. The extreme stability of the nitrogen-containing metallacyle may produce a thermodynamic gap in a hypothetical catalytic diamination. The subsequent steps of a potential catalytic cycle, namely, oxidation to the osmium(VIII) metallacycle and hydrolytic release of the diamine, are thus expected to be considerably less favorable than the analogous reactions of catalytic dihydroxylation. This also seems to be the opinion of experimentalists who reported examples of metalla-2,5-diazolidines.[3,19]

Because former computational studies focused only on the initial step of dihydroxylation, the thermodynamic-hole hypothesis requires further investigation. In the following, we present the calculated thermodynamic reaction profiles for entire catalytic cycles of the three reactions compared in this work, dihydroxylation, aminohydroxylation, and diamination. Although the mechanisms of the subsequent steps are mechanistically more complicated than the initial cycloaddition, their thermodynamics provide the first information on the feasibility of the reactions.

**Diamination versus dihydroxylation**: To identify the challenging steps in the hypothetical osmium(VIII)-catalyzed 1,2-diamination of olefins, the thermodynamic reaction profile has been predicted starting with computationally simple models. We will first discuss the analogous profile for catalytic dihydroxylation, which is used as a reference reaction. Scheme 3a shows the three steps of a simplified catalytic cycle of dihydroxylation;[26] the calculated reaction free enthalpies are presented in Table 3. In the first step, the metal oxide adds across the C=C bond (vide supra). This step is exergonic by −4 kcal mol$^{-1}$. Second, the dioxoosma-2,5-dioxolane is oxidized to a trioxoosma-2,5-dioxolane. With hydrogen peroxide as a model oxidant, this step is exergonic by as

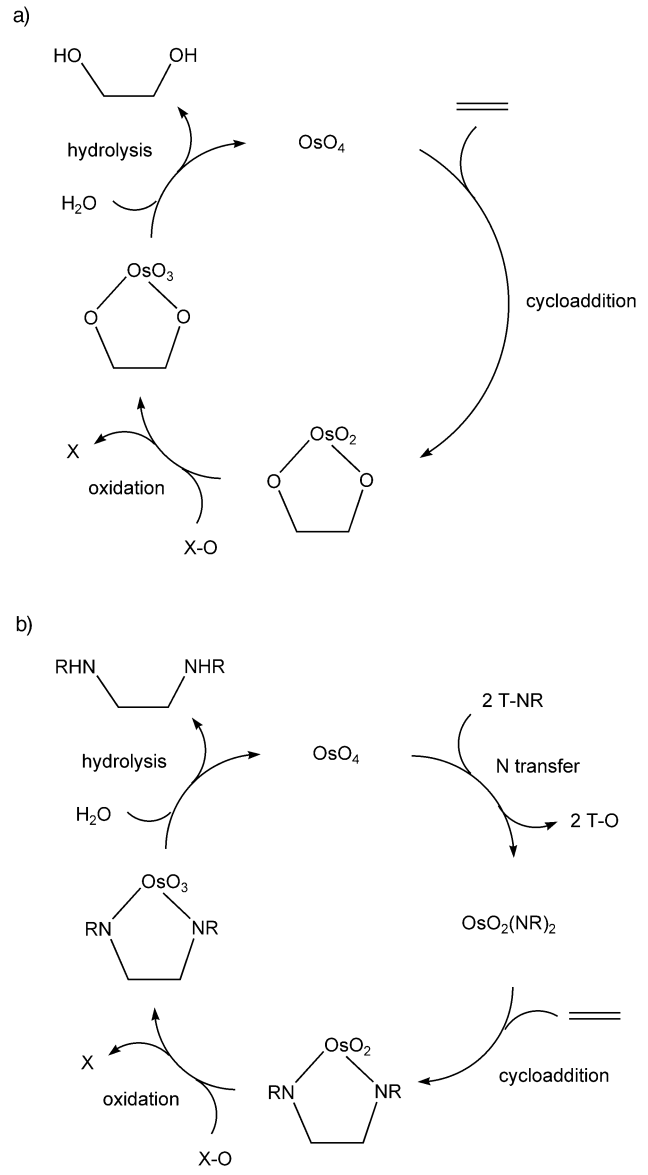


Scheme 3. Model cycles for catalytic a) dihydroxylation and b) diamination. X-O = oxidant, T-NR = imido-transfer agent.

Table 3. Calculated thermodynamic reaction profile ($\Delta G_r$) for model catalytic cycles of dihydroxylation and diamination, according to Scheme 3a and 3b. Free enthalpies relative to the corresponding reaction in the dihydroxylation cycle are also given. All values in kcal mol$^{-1}$.

| Reaction | absolute | relative to dihydrox. |
|---|---|---|
| Dihydroxylation (Scheme 3a) | | |
| $OsO_4 + C_2H_4 \rightarrow$ dioxoosma-2,5-dioxolane | −4.1 | 0.0 |
| dioxoosma-2,5-dioxolane $+ H_2O_2 \rightarrow$ triioxoosma-2,5-dioxolane $+ H_2O$ | −35.7 | 0.0 |
| triioxoosma-2,5-dioxolane $+ H_2O \rightarrow OsO_4 + (HO)CH_2CH_2(OH)$ | −18.0 | 0.0 |
| Diamination (Scheme 3b) | | |
| $OsO_2(NH)_2 + C_2H_4 \rightarrow$ dioxoosma-2,5-diazolidine | −46.2 | −42.1 |
| dioxoosma-2,5-diazolidine $+ H_2O_2 \rightarrow$ trioxoosma-2,5-diazolidine $+ H_2O$ | −24.5 | 11.2 |
| trioxoosma-2,5-diazolidine $+ H_2O \rightarrow OsO_4 + (H_2N)CH_2CH_2(NH_2)$ | −13.9 | 4.1 |
| $OsO_4 + 2NH_3 \rightarrow OsO_2(NH)_2 + 2H_2O$ | 24.4 | 24.4 |

much as −36 kcal mol$^{-1}$. Third, hydrolysis of trioxoosma-2,5-dioxolane liberates the vicinal diol and osmium tetraoxide with a theoretical reaction free enthalpy of −18 kcal mol$^{-1}$.

An analogous diamination would require the addition of the diimido complex with the C=C bond (Scheme 3b), a reaction which is shown to be more exergonic than the addition of osmium tetraoxide across C=C bonds by −42 kcal mol$^{-1}$ (Table 3). We have predicted the free enthalpies of the oxidation of the dioxoosmium(VI) metallacycles to their trioxoosmium(VIII) analogues by hydrogen peroxide.[27] Surprisingly, the oxidation of the nitrogen-containing metallacycles is less favorable than the oxidation of the oxygen-containing metallacycles by only 11 kcal mol$^{-1}$, a fraction of the difference in the reaction energies for the metalla-analogous cycloadditions. The next step of catalytic diamination, the hydrolysis of the trioxoosma-2,5-diazolidine, releases osmium tetraoxide and the diamine. Remarkably, this reaction is predicted to be less favorable than the hydrolysis of trioxoosma-2,5-dioxolane by only 4 kcal mol$^{-1}$.

The final reaction to complete the diamination cycle is oxo–imido ligand exchange. The free enthalpy of the formation of the diimido complex $OsO_2(NH)_2$ from osmium tetraoxide is calculated to be endergonic by 24 kcal mol$^{-1}$ when ammonia is used as a model nitrogen donor.[28] Now it becomes clear that the large driving force in the formation of dioxoosma-2,5-diazolidine mainly arises from the weak metal=N bond in the osmium(VIII) imido complex rather than from a stability of the metal–N bond in the osmium(VI) intermediate itself. The thermodynamic hill created by the instability of the imido complexes may be overcome by the use of activated N-transfer agents.[29]

The apparent instability of the metal=N bond is unexpected in the light of the Lewis acidity of the osmium(VIII) complexes. We have calculated the stabilization energy for the coordination of an ammine ligand with $OsO_4$, $OsO_3(NH)$, and $OsO_2(NH)_2$; the results are listed in Table 4. The binding of ammonia to osmium tetraoxide is calculated to be exothermic (by −9 kcal mol$^{-1}$) but slightly endergonic (by 3 kcal mol$^{-1}$). The theoretically predicted approximate thermoneutrality of the reaction is in agreement with an equilibrium between osmium tetraoxide and amine ligands observed spectroscopically.[30,31] Substitution of an oxo ligand by an imido ligand considerably decreases the Lewis acidity. The coordination of ammonia to imidotrioxoosmium is calculated to be less favorable (by 3 kcal mol$^{-1}$ relative to $OsO_4$, see Table 4), whereas no stable structure of $[OsO_2(NH)_2(NH_3)]$ has been obtained with the ammine ligand in the first coordination sphere. The trend in the Lewis acidity of the osmium(VIII) complexes is corroborated by calculated atomic partial charges listed in Table 5. The change at the metal successively decreases from 2.20 in $OsO_4$ to 1.89 in $OsO_2(NH)_2$. It is important to note that the weak Lewis acidity of the bisimido complexes implies that the traditional concept of transferring stereochemical information by coordination of

  

Table 4. Lewis acidity of osmium(VIII) imido and oxo complexes. Stabilization energies ($\Delta E_r$) calculated at the B3LYP/III+//B3LYP/II level and free enthalpies ($\Delta G_a$, $\Delta G_r$) at 298.15 K for the coordination of $NH_3$ to $OsO_4$, $OsO_3(NH)$, and $OsO_2(NH)_2$. All values in kcal mol$^{-1}$.

| Reaction | $\Delta E_r$ | $\Delta G_r$ |
|---|---|---|
| $OsO_4 + NH_3 \rightarrow [OsO_4(NH_3)]$ | −8.6 | 2.6 |
| $OsO_3(NH) + NH_3 \rightarrow$ *cis*-$[OsO_3(NH)(NH_3)]$ | −3.6 | 7.8 |
| $OsO_3(NH) + NH_3 \rightarrow$ *trans*-$[OsO_3(NH)(NH_3)]$ | −5.8 | 5.9 |
| $OsO_2(NH)_2 + NH_3 \rightarrow$ *cis*-$[OsO_2(NH)_2(NH_3)]$ | –[a] | – |
| $OsO_2(NH)_2 + NH_3 \rightarrow$ *trans*-$[OsO_2(NH)_2(NH_3)]$ | –[a] | – |

[a] The ammine ligand is displaced from the first coordination shell.

Table 5. Calculated NPA charges of selected intermediates.

| Molecule | Os | O Os=O | N Os=N | O cycle | N cycle | $C_2H_4$[a] cycle |
|---|---|---|---|---|---|---|
| $OsO_4$ | 2.20 | −0.55 | | | | |
| $OsO_3(NH)$ | 2.05 | −0.56 | −0.75 | | | |
| $OsO_2(NH)_2$ | 1.89 | −0.59 | −0.73 | | | |
| diimidoosma-2,5-dioxolane | 1.59 | | −0.73 | −0.70 | | 0.56 |
| dioxoosma-2,5-dioxolane | 2.13 | −0.58 | | −0.81 | | 0.64 |
| trioxoosma-2,5-dioxolane | 2.12 | −0.48 | | −0.67 | | 0.64 |
| dioxoosma-2,5-diazolidine | 1.71 | −0.65 | | | −0.77 | 0.37 |
| trioxoosma-2,5-diazolidine | 1.98 | −0.54 | | | −0.77 | 0.39 |

[a] Sum of the charges at the C and H atoms of the ethylene moiety.

chiral ligands,[3] such as cinchona alkaloids, will probably not succeed in case of diamination. Therefore, alternative concepts should be explored, for instance, incorporating chiral auxiliaries in the substrate.[19]

To rationalize the apparent discrepancy between the weaker Lewis acidity of the imido complexes and the relative instability of Os=N bond, an energy decomposition analysis of $OsO_4$ and $OsO_3(NH)$ has been performed. The bonds have been analyzed in terms of $OsO_3^{2+}$ interacting with $O^{2-}$ and $NH^{2-}$, respectively, to give partial triple bonds (Table 6). Because the $C_s$-symmetric structure of $OsO_3(NH)$ with a bent imido ligand is found to be more stable than a $C_{3v}$-symmetric structure with a linear imido ligand by only 0.2 kcal mol$^{-1}$,[32] the latter has been considered for group-theoretical reasons.[21] The analysis shows a larger bond energy and a much stronger electrostatic component $\Delta E_{elst}$ for $OsO_4$ (Table 6). In contrast, the stabilizing orbital-interaction energy $\Delta E_{orb}$ is significantly stronger in $OsO_3(NH)$, indicating the more covalent nature of the imido bond compared to the oxo bond. The contributions from the $a_1$ and $e$ symmetry orbitals to $\Delta E_{orb}$ show that $O^{2-}$ is a slightly stronger σ donor but a much weaker π donor than $(NH)^{2-}$ (Figure 3). The σ/π ratio is approximately 1:1 in the Os=O bond and 2:3 in the Os=NH bond. It is the greater covalence in the metal=N bonds which decreases the Lewis acidity of the imido complexes, although the stronger electrostatics in osmium tetraoxide cause the larger stability of the Os=O bond.

Table 6. Electrostatic versus covalent nature of oxo and imido-osmium(VIII) bonds. Energy decomposition of the Os=O and Os=NH bonds in $C_{3v}$-symmetric $OsO_4$ and $OsO_3(NH)$, respectively, at the BLYP/IV′ level. Bold: contributions of the $\Gamma_i$ symmetry orbitals to the stabilizing orbital-interaction energy $\Delta E_{orb}$. All energies in kcal mol$^{-1}$.

| Contribution | $\Gamma_i$ | $OsO_4$ | $OsO_3(NH)$[a] |
|---|---|---|---|
| $\Delta E_{str}$ $O^{2-}$ or $NH^{2-}$ | | 0.0 | 1.8 |
| $\Delta E_{str}$ $OsO_3^{2+}$ | | 5.2 | 5.7 |
| $\Delta E_{str}$ total | | 5.2 | 7.5 |
| $\Delta E_{Pauli}$ | | 539.0 | 492.4 |
| $\Delta E_{elst}$ | | −1101.7 | −1011.3 |
| $\Delta E_{orb}$ | | −425.7 | −452.6 |
| $\boldsymbol{\Delta E_{orb}(\Gamma_i)}$ | $\boldsymbol{a_1}$ | **−196.0** | **−173.6** |
| | $\boldsymbol{a_2}$ | **−1.2** | **−1.2** |
| | $\boldsymbol{e}$ | **−228.6** | **−277.8** |
| $\Delta E_{int} = \Delta E_{Pauli} + \Delta E_{elst} + \Delta E_{orb}$ | | −988.4 | −971.5 |
| $\Delta E = \Delta E_{str} + \Delta E_{int}$ | | −983.2 | −964.0 |
| $\Delta E_{orb}/\Delta E_{elst}$ | | 0.39 | 0.45 |
| $\Delta E_{orb}(a_1)/\Delta E_{orb}(e)$ | | 0.86 | 0.62 |

[a] A $C_s$-symmetric structure of $OsO_3(NH)$ with a bent imido ligand (Os-N-H angle 135.4) is more stable by 0.2 kcal mol$^{-1}$.

**Steric and electronic control of thermodynamic profiles**: Although the oxidation of dioxoosma-2,5-diazolidines is less favorable than the oxidation of dioxoosma-2,5-oxolanes by "only" 11 kcal mol$^{-1}$, decreasing this difference by modifying the metallaazacycles remains a challenge on account of the structural similarity of the dioxo and trioxo species. To explore concepts of controlling the relative stability of the dioxo- and trioxoosma-2,5-diazolidines, we have compared their atomic partial charges to those in the corresponding metallaoxacycles (Table 5). The calculations show that the charge at the metal in the dioxo- and trioxo-2,5-dioxolanes remains very high (2.13 and 2.12), almost as high as the metal charge in osmium tetraoxide (2.20). In contrast, the charge at the metal in $OsO_2(NH)_2$ (1.89) decreases upon NH=Os=NH addition to ethylene (1.71), and increases in turn upon oxidation (1.98). The charge of the ethylene moiety in the metallaoxacycles (0.64) is more positive than that in the metallaazacycles (0.37 and 0.39). If the electronic structure of the metallaoxacycles represents a constellation for a successful oxidative catalytic cycle, electron-withdrawing substituents on the metallaazacycles are anticipated to improve the thermodynamics of the oxidation.

To investigate how the free enthalpies of the reaction steps can be controlled, we have predicted the effect of modifications in the substrate ($CH_2$=CHR′) on the free enthalpies of the catalytic reaction (see Supporting Information, Table S1). Electron-deficient C=C double bonds are represented by acrolein (R′ = CHO), electron-rich C=C double bonds by propylene (R′ = Me). The calculations predict rel-

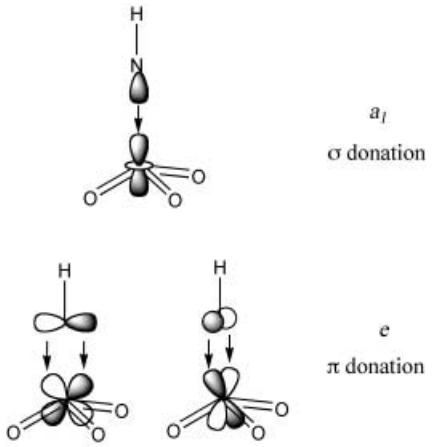


Figure 3. $a_1$ and $e$ symmetry orbitals in $C_{3v}$-symmetric $OsO_4$ and $OsO_3(NH)$.

atively small changes in the thermodynamic reaction profile when compared to the reactions of ethylene (R′ = H), with the greatest change being the destabilization of dioxoosma-2,5-diazolidine in the case of acrolein by 5 kcal mol$^{-1}$.

In contrast, the results presented in Table 7 reveal that steric and electronic effects of the imido substituents R open up a much larger potential of controlling the thermodynamic reaction profile. The important free enthalpies relative to the corresponding reactions in dihydroxylation are displayed in Figure 4. The [3+2] cycloaddition of bis(methylimido)dioxoosmium(VIII) to ethylene is less exergonic than the addition of $OsO_2(NH)_2$ by 11 kcal mol$^{-1}$; nevertheless, this reaction step remains the most exergonic of the entire cycle (Table 7). As expected from the calculated atomic charges (vide supra), the oxidation of the dioxoosmium(VI) species to the trioxoosmium(VIII) species is less favorable in case of R = Me, by 6 kcal mol$^{-1}$. The free enthalpy of hydrolysis is the same for the imido and methylimido complexes. While the oxo–imido exchange was predicted to be strongly endergonic (with ammonia as a model nitrogen donor), the analogous reaction with R = Me is endergonic by only 2 kcal mol$^{-1}$ (Table 7).

A comparison of the thermodynamic reaction profile for R = Me and R = *tert*-butyl provides a measure of steric effects (Figure 4, Table 7). The formation of $[OsO_2(NR)_2]$ from $OsO_4$ remains unaffected by steric strain, because the reaction free enthalpies for R = Me and *tert*-Bu are approximately equal. In contrast, the cycloaddition of $OsO_2(NR)_2$ is 13 kcal mol$^{-1}$ less favorable for R = *t*Bu. Moreover, the oxidation of the dioxoosma-2,5-diazolidine is less favorable by additional 15 kcal mol$^{-1}$, accumulating a total steric strain of 28 kcal mol$^{-1}$ in the trioxoosma-2,5-diazolidine. Partial relief of steric strain renders subsequent hydrolysis more exergonic by −17 kcal mol$^{-1}$ compared to that of the methyl derivative.

Electron-withdrawing trifluoromethyl groups at the imido moieties strongly disfavor oxo–imido exchange by 11 kcal mol$^{-1}$ relative to R = H, showing the opposite trend to that of electron-releasing methyl groups. Cycloaddition is preferred by −3 kcal mol$^{-1}$ relative to R = H, but subsequent oxidation is less exergonic than that for R = H by 13 kcal mol$^{-1}$ and even less exergonic than that for R = Me by 8 kcal mol$^{-1}$, indicating a considerable amount of steric strain induced by $CF_3$ substituents.

In summary, steric effects disfavor cycloaddition, strongly disfavor oxidation, slightly favor hydrolysis, and do not significantly affect oxo–imido exchange. Electron-releasing groups at the imido ligands disfavor cycloaddition, slightly disfavor oxidation, do not significantly affect hydrolysis, and strongly favor oxo–imido exchange. In principle, the opposite electronic effects can be induced by electron-withdrawing groups at the imido ligands, but steric effects may mask electronic effects in the reactions of the metallacycles.

Table 7. Electronic and steric ligand control of the diamination model cycle. Calculated thermodynamic reaction profile ($\Delta G_r$) for ethylene diamination with $OsO_2(NR)_2$ (R = Me, *t*Bu, $CF_3$), according to Scheme 3b. All values in kcal mol$^{-1}$.

| Reaction | Absolute | Relative to dihydrox. | Relative to R = H |
|---|---|---|---|
| R = Me | | | |
| $OsO_2(NR)_2 + C_2H_4 \rightarrow$ dioxoosma-2,5-diazolidine | −35.1 | −31.0 | 11.1 |
| dioxoosma-2,5-diazolidine + $H_2O_2 \rightarrow$ trioxoosma-2,5-diazolidine + $H_2O$ | −18.8 | 16.9 | 5.7 |
| trioxoosma-2,5-diazolidine + $H_2O \rightarrow OsO_4$ + $(NHR)CH_2CH_2(NHR)$ | −13.3 | 4.7 | 0.6 |
| $OsO_4 + 2\,RNH_2 \rightarrow OsO_2(NR)_2 + 2\,H_2O$ | 2.4 | 2.4 | −22.0 |
| R = *t*Bu | | | |
| $OsO_2(NR)_2 + C_2H_4 \rightarrow$ dioxoosma-2,5-diazolidine | −22.5 | −18.4 | 23.7 |
| dioxoosma-2,5-diazolidine + $H_2O_2 \rightarrow$ trioxoosma-2,5-diazolidine + $H_2O$ | −4.1 | 31.6 | 20.4 |
| trioxoosma-2,5-diazolidine + $H_2O \rightarrow OsO_4$ + $(NHR)CH_2CH_2(NHR)$ | −31.0 | −13.0 | −17.1 |
| $OsO_4 + 2\,RNH_2 \rightarrow OsO_2(NR)_2 + 2\,H_2O$ | 0.6 | 0.6 | −23.8 |
| R = $CF_3$ | | | |
| $OsO_2(NR)_2 + C_2H_4 \rightarrow$ dioxoosma-2,5-diazolidine | −49.4 | −45.3 | −3.2 |
| dioxoosma-2,5-diazolidine + $H_2O_2 \rightarrow$ trioxoosma-2,5-diazolidine + $H_2O$ | −11.1 | 24.6 | 13.4 |
| trioxoosma-2,5-diazolidine + $H_2O \rightarrow OsO_4$ + $(NHR)CH_2CH_2(NHR)$ | −38.2 | −20.2 | −24.3 |
| $OsO_4 + 2\,RNH_2 \rightarrow OsO_2(NR)_2 + 2\,H_2O$ | 35.7 | 35.7 | 11.3 |

**Diamination versus aminohydroxylation:** In state-of-the-art protocols for catalytic aminohydroxylation, oxidation and nitrogen transfer are typically combined in a single step.[4] Nitrogen sources include *N*-halo amides derived from sulfonamides, carbamates, amides, and nitrogen heterocycles,[4c–e,33] which oxidize dioxoosma-2,5-oxazolidines to imidodioxoosma-2,5-oxazolidines (Scheme 4a). Theory predicts the initial cycloaddition of the NH=Os=O

  

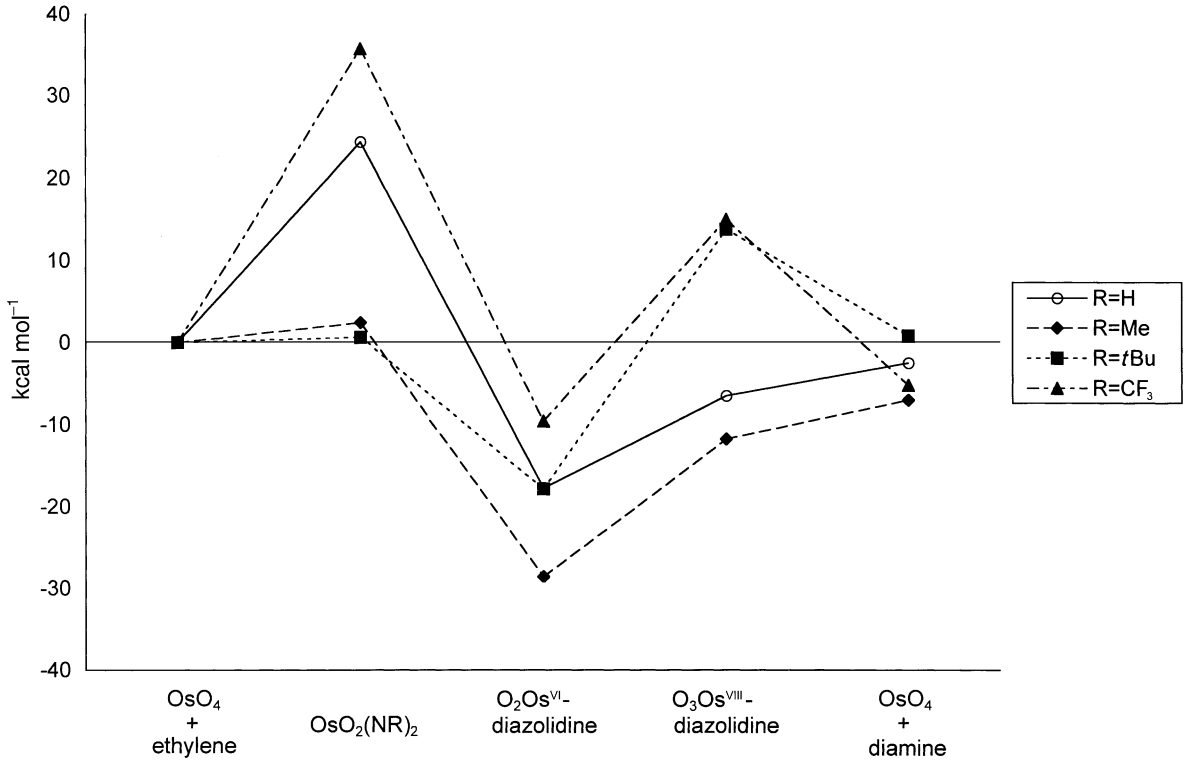


Figure 4. Thermodynamic reaction profile for $OsO_2(NR)_2$-catalyzed diamination according to Scheme 3b relative to that of dihydroxylation (zero line) shown in Scheme 3a. Free enthalpies in kcal mol$^{-1}$.

moiety to ethylene to be exergonic by $-25$ kcal mol$^{-1}$, which lies between the reaction free enthalpies for less exergonic O=Os=O additions and more exergonic NH=Os=NH additions (vide supra). The second step, oxidative imido transfer was studied with the simple model N-transfer agent chloroamine ($RNH_2Cl$, here R = H) and has a reaction free enthalpy of 15 kcal mol$^{-1}$. Note that this value can easily be rendered exothermic by the choice of the nitrogen source. The discussion again focuses on relative reaction free enthalpies, which do not depend on the nitrogen source. Hydrolysis, the third and last step of aminohydroxylation according to Scheme 4a, is calculated to be exergonic by $-14$ kcal mol$^{-1}$, which seems a typical value for the hydrolysis of the metallacycles.

This reaction profile for aminohydroxylation according to Scheme 4a is used as a reference in the evaluation of an analogous scenario for diamination according to Scheme 4b.[34] Free enthalpies relative to the corresponding reactions in aminohydroxylation are visualized in Figure 5 (for the values, see Tables S2 and S3 in the Supporting Information). While cycloaddition is more favorable in the latter case by $-21$ kcal mol$^{-1}$ (R = H), oxidative nitrogen transfer is less favorable by 8 kcal mol$^{-1}$. Since the hydrolysis of the imidodioxoosma-2,5-diazolidines yields the diamine and imidotrioxoosmium(VIII), diamination according to Scheme 4b requires an additional non-oxidative nitrogen transfer step giving diimidodioxoosmium(VIII) in a 13 kcal mol$^{-1}$ endergonic reaction (with ammonia as the N-transfer agent).

Substituents on the imido ligands are found to induce steric and electronic effects in a very similar manner as that shown in the catalytic model cycle in Scheme 3b and Figure 4 discussed in the former section. However, the changes in free reaction enthalpies appear less dramatic when diamination (Scheme 4b) is compared to aminohydroxylation (Scheme 4a) with the same imido substituent R because the effects are already partly present in the latter reactions. This can be impressively demonstrated by comparing the thermodynamic profiles relative to dihydroxylation and aminohydroxylation shown in Figure 4 and 5, respectively, with the latter showing the same patterns as the former but reaching only half of the magnitude.

## Conclusion

The osmium-catalyzed dihydroxylation and aminohydroxylation of olefins provide an elegant route to 1,2-functionalized compounds, but an analogous diamination remains a holy grail. This challenge was the motivation for a density functional study on the reaction of oxo-imido osmium(VIII) complexes with C=C bonds and the subsequent steps of as-yet hypothetical catalytic reaction courses. Catalytic model cycles have been designed for diamination, which are based on the counterparts of the frequently used dihydroxylation and aminohydroxylation methods. The catalytic cycles consist of five modules: 1) cycloaddition, 2) hydrolysis, 3) oxygen transfer, 4) oxidative nitrogen transfer, and 5) oxo–imido exchange. The results of this work can be summarized as follows:

1) Theory predicts a chemoselective and perispecific [3+2] addition of the NH=Os=NH moiety of diimidodioxoos-

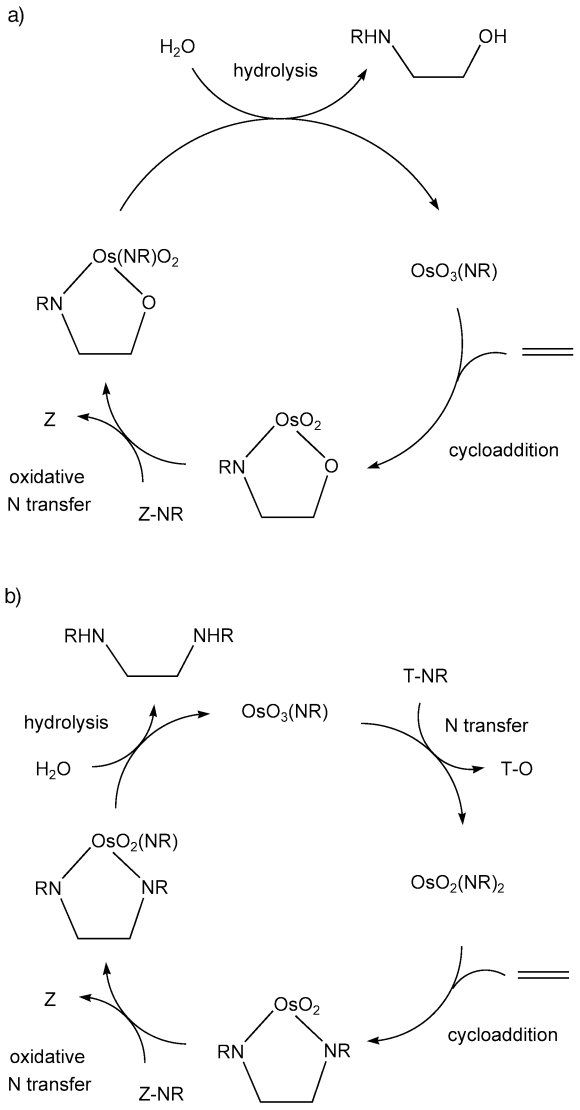


Scheme 4. Model cycles for catalytic a) aminohydroxylation, and b) diamination. Z-NR = oxidative imido-transfer agent, T-NR = non-oxidative imido-transfer agent.

mium(VIII) to ethylene. An analysis of the activation energies for the [3+2] additions of the NH=Os=NH and O=Os=O moieties shows both reactions to be orbital-controlled and identifies two important factors governing chemoselectivity: first, elongation of the Os=NH groups toward the transition state geometry requires less energy than the elongation of the Os=O bonds. Second, decomposition of the stabilizing orbital interactions into the contributions from symmetry orbitals indicates that the energy contribution of π backdonation from the imido ligands to the π* orbital of the olefin is particularly enhanced in the NH=Os=NH addition.

2) The thermodynamic reaction profile for a catalytic model cycle of diamination including cycloaddition, oxidation, hydrolysis, and oxo–imido exchange has been determined and compared to the profiles for osmium-catalyzed dihydroxylation (Scheme 3b versus 3a). The [3+2] cycloaddition of NH=Os(O)$_2$=NH to ethylene is more exergonic than the corresponding reaction in dihydroxylation by $-42$ kcal mol$^{-1}$. Surprisingly, this large free enthalpy difference does not cause a deep thermodynamic hole because the subsequent oxidation of the osmium(**VI**) azacycles to the osmium(**VIII**) azacycles is less exothermic than the corresponding oxidation of the osmium(**VI**) oxacycles in catalytic dihydroxylation by only 11 kcal mol$^{-1}$. Moreover, the free enthalpies of the hydrolytic release of the products from the osmium(**VIII**) cycles differ by only 4 kcal mol$^{-1}$. The endergonic formation of diimidodioxoosmium(**VIII**) from osmium tetraoxide, which is not required in the parent dihydroxylation, creates an intrinsic thermodynamic hill of 24 kcal mol$^{-1}$ (calculated versus $NH_3/H_2O$) to be bulldozed by the use of activated nitrogen sources. Despite the instability of the Os=N bonds (relative to the Os=O bonds), their greater covalence decreases the Lewis acidity of the metal, depriving diimidodioxoosmium(**VIII**) of the ability to bind additional ligands that could have been used for transferring chiral information in a stereoselective diamination.
3) Substituents on the imido ligands control the thermodynamic reaction profile for the hypothetical diamination to a very large extent. Electron-releasing methyl groups on the nitrogen atoms render the oxidation of the dioxoosma-2,5-diazolidine to the trioxo species slightly less preferred, but significantly favor oxo–imido exchange. Electron-withdrawing trifluoromethyl groups destabilize imidotrioxoosmium(**VIII**) and stabilize the dioxoosma-2,5-diazolidine. Steric effects induced by bulky *tert*-butyl groups particularly destabilize the trioxoosmium(**VIII**) azacycle relative to the dioxoosmium(**VI**) azacycle. Substituents in the substrate can, in principle, change the free enthalpies of the model cycle in a similar manner, but their effect is smaller than that induced by N-substitution by an order of magnitude.
4) The thermodynamic reaction profile for an alternative catalytic model cycle of diamination including cycloaddition, oxidative N transfer, hydrolysis, and oxo–imido exchange has also been evaluated and compared to the profile for osmium-catalyzed aminohydroxylation (Scheme 4b versus 4a). The free enthalpies of the four reaction steps relative to those in aminohydroxylation are predicted to be $-20$ kcal mol$^{-1}$, 8 kcal mol$^{-1}$, 0 kcal mol$^{-1}$, and 12 kcal mol$^{-1}$, identifying oxidative and non-oxidative N transfer as the greatest challenges. Electron-releasing groups at the imido ligands particularly favor the non-oxidative N-transfer event, whereas the presence of sterically demanding substituents increase the free enthalpy of oxidative N transfer.

## Computational Methods

The geometries of the molecules and transition states (TS) were optimized at the gradient-corrected DFT level with the 3-parameter fit of exchange and correlation potentials introduced by Becke (B3LYP),[35] as implemented in Gaussian 98.[36] Shape-consistent quasirelativistic small-core ECPs[37] and a (441/2111/21) valence-basis set were employed for Os, while 6-31G(d) all-electron basis sets were used for the other atoms.[38] This basis-set combination is denoted II.[39] Vibrational frequen-

  

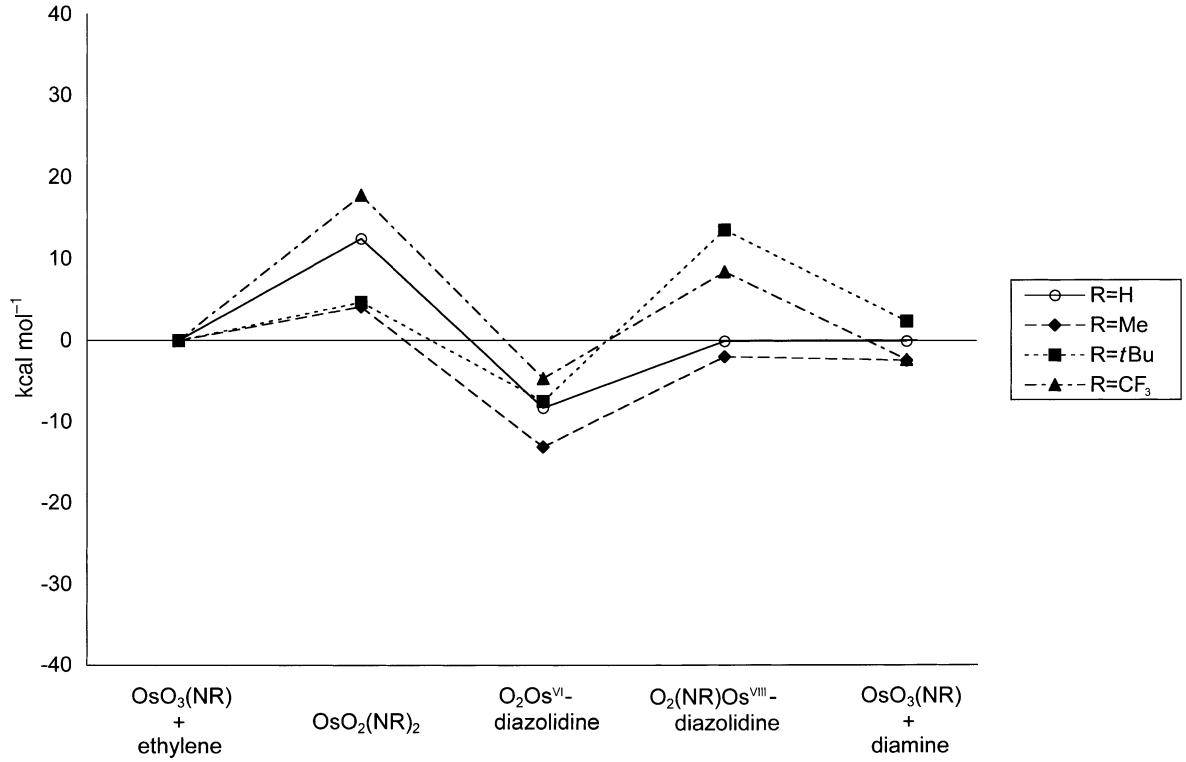


Figure 5. Thermodynamic reaction profile for $OsO_2(NR)_2$-catalyzed diamination according to Scheme 4b relative to that of aminohydroxylation (zero line) shown in Scheme 4a. Free enthalpies in kcal mol$^{-1}$.

cies and zero-point energies (ZPE) were also calculated at the B3LYP/II level. All structures reported here are either minima (NIMAG = 0) or transition states (NIMAG = 1) on the potential energy surfaces. Improved total energies were calculated at the B3LYP level with the same ECP and valence-basis set at the metals, but totally uncontracted and augmented with a set of f functions,[40] together with a 6-311+G(d,p) basis set for the other atoms. This basis-set combination is denoted III+. Unless otherwise mentioned, the values discussed in the text are activation and reaction free enthalpies ($\Delta G_a$, $\Delta G_r$), also denoted Gibbs free energies. These were calculated by adding corrections from zero-point energy (ZPE), thermal energy, work, and entropy evaluated at the B3LYP/II level at 298.15 K to the activation and reaction energies ($\Delta E_a$, $\Delta E_r$), which were calculated at the B3LYP/III+//II level. Single-point calculations of selected molecules at the CCSD(T)/III+//B3LYP/II level using the coupled-cluster-singles-doubles method with perturbative triples[41,42] show very good agreement of relative energies with those at the B3LYP/III+//II level (Supporting Information). *tert*-Butyl substituents were considered by means of the STO-3G basis set at the terminal methyl groups for optimization, and the 6-31G(d) basis set was used for calculating improved energies. Atomic partial charges were predicted with the NPA scheme.[43]

Energy decomposition analyses were performed at the BLYP level[44,45] as implemented in the Amsterdam Density Functional 2002 program (ADF).[46] Scalar-relativistic effects were considered by the zeroth-order regular approximation (ZORA).[47] Uncontracted Slater-type orbitals (STOs) were used as basis functions.[48] The valence basis functions at Os have triple-$\zeta$ quality, augmented with a set of p and f functions. The valence basis set at the other atoms has triple-$\zeta$ quality, augmented with a set of d functions. The $(1s)^2$ core electrons of C, N, and O and the $(1s\,2sp\,3spd\,4spdf)^{60}$ core electrons of Os were treated within the frozen-core approximation.[49] The structures to be investigated are divided into two fragments. If the structure of interest is a metal complex, the stabilization energy $\Delta E_r$ is decomposed; if it is a transition state, the activation energy $\Delta E_a$ is decomposed. $\Delta E_a$ (or $\Delta E_r$) is the sum of two contributions, strain energy $\Delta E_{str}$ and interaction energy $\Delta E_{int}$ ($\Delta E_a$ (or $\Delta E_r$) = $\Delta E_{str}$ + $\Delta E_{int}$). Strain energy $\Delta E_{str}$ is the difference between the energy of the isolated fragments in the geometry of the complex or transition state and the sum of the energy of the two fragments in their equilibrium geometry. $\Delta E_{int}$, which is the energy of interaction between the fragments, can in turn be partitioned into three components ($\Delta E_{int} = \Delta E_{elst} + \Delta E_{Pauli} + \Delta E_{orb}$). $\Delta E_{elst}$ gives the electrostatic interaction energy between the fragments, which is calculated with a frozen electron-density distribution in the geometry of the complex or TS. Pauli repulsion ($\Delta E_{Pauli}$) considers the energy required for antisymmetrization and re-normalization of the Kohn–Sham orbitals of the superimposing fragments. $\Delta E_{Pauli}$ represents the repulsive interaction energy between the fragments which is caused by the fact that two electrons with the same spin cannot occupy the same region in space (Pauli principle). Finally, the stabilizing orbital-interaction term $\Delta E_{orb}$ is calculated with the Kohn–Sham orbitals relaxing to their optimal form.

## Acknowledgement

This work is a co-contribution from the Swiss Center for Scientific Computing, CSCS, ETH Zürich, 6928 Manno (Switzerland). D.V.D thanks Michele Parrinello for support. We thank the Fonds der Chemischen Industrie and the Federal Ministry of Education and Research (Germany) for Liebig Fellowships to both authors and for organizing the Steinheimer discussions. We also thank the staff at the computing centers CSCS Manno and HLR Marburg for providing an excellent service.

[1] F. Fache, E. Schulz, M. L. Tommasino, M. Lemaire, *Chem. Rev.* **2000**, *100*, 2159.
[2] a) B. Lippert, *Cisplatin*, Wiley-VCH, Weinheim, **1999**; b) E. Wong, C. M. Giandomenico, *Chem. Rev.* **1999**, *99*, 2451.
[3] D. Lucet, T. Le Gall, C. Mioskowski, *Angew. Chem.* **1998**, *110*, 2724; *Angew. Chem. Int. Ed.* **1998**, *37*, 2580.
[4] Reviews: a) M. Schröder, *Chem. Rev.* **1980**, *80*, 187; b) H. C. Kolb, M. S. Van Nieuwenhze, K. B. Sharpless, *Chem. Rev.* **1994**, *94*, 2483; c) H. C. Kolb, K. B. Sharpless, in *Transition Metals for Fine Chemicals and Organic Synthesis, Vol. 2*, (Eds.: M. Beller, C. Bolm),

Wiley-VCH, Weinheim, **1998**, pp. 243; d) C. Bolm, J. P. Hildebrand, K. Muñiz in *Catalytic Asymmetric Synthesis* (Ed.: I. Ojima), Wiley-VCH: Weinheim, **2000**, 2nd ed., pp. 399; e) J. A. Bodkin, M. D. McLoad, *J. Chem. Soc. Perkin Trans. 1* **2002**, 2746; f) K. B. Sharpless, *Angew. Chem.* **2002**, *114*, 2126; *Angew. Chem. Int. Ed.* **2002**, *41*, 2024.

[5] S. G. Hentges, K. B. Sharpless, *J. Am. Chem. Soc.* **1980**, *102*, 4263.

[6] G. Li, H.-T. Chang, K. B. Sharpless, *Angew. Chem.* **1996**, *108*, 449; *Angew. Chem. Int. Ed. Engl.* **1996**, *35*, 451.

[7] Recent developments: a) C. Döbler, G. Mehltretter, U. Sundermeier, M. Beller, *J. Am. Chem. Soc.* **2000**, *122*, 10289; b) S. Y. Jonsson, K. Färnegårdh, J.-E. Bäckvall, *J. Am. Chem. Soc.* **2001**, *123*, 1365; c) A. Severeyns, D. E. De Vos, L. Fiermans, F. Verpoort, P. J. Grobet, P. A. Jacobs, *Angew. Chem.* **2001**, *113*, 606; *Angew. Chem. Int. Ed.* **2001**, *40*, 586; d) V. V. Fokin, K. B. Sharpless, *Angew. Chem.* **2001**, *113*, 3563; *Angew. Chem. Int. Ed.* **2001**, *40*, 3455; e) C=C cleavage: B. R. Travis, R. S. Narayan, B. Borhan, *J. Am. Chem. Soc.* **2002**, *124*, 3824; f) B. M. Choudary, N. S. Chowdari, K. Jyothi, M. L. Kantam, *J. Am. Chem. Soc.* **2002**, *124*, 5341; g) T. J. Donohoe, P. D. Johnson, A. Cowley, M. Keenan, *J. Am. Chem. Soc.* **2002**, *124*, 12934; h) M. A. Andersson, R. Epple, V. V. Fokin, K. B. Sharpless, *Angew. Chem.* **2002**, *114*, 490; *Angew. Chem. Int. Ed.* **2002**, *41*, 472; i) R. A. Bhunnoo, Y. L. Hu, D. I. Laine, R. C. D. Brown, *Angew. Chem.* **2002**, *114*, 3629; *Angew. Chem. Int. Ed.* **2002**, *41*, 3479; j) K. Lee, Y.-H. Kim, S. B. Han, H. Kang, S. Park, W. S. Seo, J. T. Park, B. Kim, S. Chang, *J. Am. Chem. Soc.* **2003**, *125*, 6844; k) S. Y. Jonsson, H. Adolfsson, J.-E. Bäckvall, *Chem. Eur. J.* **2003**, *9*, 2665.

[8] A. O. Chong, K. Oshima, K. B. Sharpless, *J. Am. Chem. Soc.* **1977**, *99*, 3420.

[9] D. V. Deubel, G. Frenking, *Acc. Chem. Res.* **2003**, *36*, 645.

[10] D. V. Deubel, S. Schlecht, G. Frenking, *J. Am. Chem. Soc.* **2001**, *123*, 10085.

[11] a) D. V. Deubel, G. Frenking, *J. Am. Chem. Soc.* **1999**, *121*, 2021; b) D. V. Deubel, J. Sundermeyer, G. Frenking, *J. Am. Chem. Soc.* **2000**, *122*, 10101; c) D. V. Deubel, *Angew. Chem.* **2003**, *115*, 2019; *Angew. Chem. Int. Ed.* **2003**, *42*, 1974; d) D. V. Deubel, *J. Am. Chem. Soc.* **2003**, *125*, 15308; e) D. V. Deubel, *J. Am. Chem. Soc.* **2004**, *126*, 996.

[12] a) U. Pidun, C. Boehme, G. Frenking, *Angew. Chem.* **1996**, *108*, 3008; *Angew. Chem. Int. Ed. Engl.* **1996**, *35*, 2817; b) S. Dapprich, G. Ujaque, F. Maseras, A. Lledós, D. G. Musaev, K. Morokuma, *J. Am. Chem. Soc.* **1996**, *118*, 11660; c) M. Torrent, L. Deng, M. Duran, M. Sola, T. Ziegler, *Organometallics* **1997**, *16*, 13; d) A. J. Del Monte, J. Haller, K. N. Houk, K. B. Sharpless, D. A. Singleton, T. Strassner, A. A. Thomas, *J. Am. Chem. Soc.* **1997**, *119*, 9907; e) G. Ujaque, F. Maseras, A. Lledós, *Eur. J. Org. Chem.* **2003**, 833;

[13] Theoretical studies on the stereoselective [3+2] addition: a) G. Ujaque, F. Maseras, A. Lledós, *J. Am. Chem. Soc.* **1999**, *121*, 1317; b) P. A. Norrby, T. Rasmussen, J. Haller, T. Strassner, K. N. Houk, *J. Am. Chem. Soc.* **1999**, *121*, 10186; c) P. Fristrup, D. Tanner, P.-O. Norrby, *Chirality* **2003**, *15*, 360.

[14] a) W. A. Herrmann, F. E. Kühn, *Acc. Chem. Res.* **1997**, *30*, 169; b) C. C. Romão, F. E. Kühn, W. A. Herrmann, *Chem. Rev.* **1997**, *97*, 3197.

[15] K. P. Gable, F. A. Zhuravlev, *J. Am. Chem. Soc.* **2002**, *124*, 3970.

[16] X. Chen, X. Zhang, P. Chen, *Angew. Chem.* **2003**, *115*, 3928; *Angew. Chem. Int. Ed.* **2003**, *42*, 3798.

[17] K. Muñiz, M. Nieger, H. Mansikkamäki, *Angew. Chem.* **2003**, *115*, 6143; *Angew. Chem. Int. Ed.* **2003**, *43*, 5958.

[18] See: a) P. Gisdakis, N. Rösch, *J. Am. Chem. Soc.* **2001**, *123*, 697; b) D. V. Deubel, T. Ziegler, *Organometallics* **2002**, *21*, 4432.

[19] a) K. Muñiz, M. Nieger, *Synlett* **2003**, 211; b) K. Muñiz, A. Iesato, M. Nieger, *Chem. Eur. J.* **2003**, *9*, 5581.

[20] a) K. Morokuma, *J. Chem. Phys.* **1971**, *55*, 1236; b) T. Ziegler, A. Rauk, *Theor. Chim. Acta* **1977**, *46*, 1.

[21] Reviews: a) F. M. Bickelhaupt, E. J. Baerends, *Rev. Comput. Chem.* **2000**, *15*, 1; b) G. Frenking, N. Fröhlich, *Chem. Rev.* **2000**, *100*, 717; c) G. Frenking, K. Wichmann, N. Fröhlich, C. Loschen, M. Lein, J. Frunzke, V. M. Rayón, *Coord. Chem. Rev.* **2003**, *238*, 55.

[22] F. M. Bickelhaupt, R. L. DeKock, E. J. Baerends, *J. Am. Chem. Soc.* **2002**, *124*, 1500.

[23] See: a) D. V. Deubel, *J. Am. Chem. Soc.* **2002**, *124*, 5834; b) D. V. Deubel, *J. Am. Chem. Soc.* **2002**, *124*, 12312.

[24] D. V. Deubel, *J. Phys. Chem. A* **2002**, *106*, 431.

[25] D. V. Deubel, *J. Phys. Chem. A* **2001**, *105*, 4765.

[26] Osmate esters can be stabilized by the coordination of additional ligands and by the formation of metallabicycles; see ref. [4] for details.

[27] For an assessment of the oxygen-transfer potential of several oxidants, see: R. D. Bach, P. Y. Ayala, H. B. Schlegel, *J. Am. Chem. Soc.* **1996**, *118*, 12758.

[28] To compare relative free enthalpies of the reactions, which do not depend on the oxygen or nitrogen source, we have consistently investigated the reactions with simple model compounds, that is, with $H_2O_2$ as the O donor, chloroamines RNHCl as the oxidative N donor, and amines $RNH_2$ as the non-oxidative N donor.

[29] a) W. A. Nugent, R. L. Harlow, R. J. McKinney, *J. Am. Chem. Soc.* **1979**, *101*, 7265; b) A. A. Danopoulos, G. Wilkinson, B. Hussain-Bates, M. B. Hursthouse, *J. Chem. Soc. Dalton Trans.* **1991**, 269.

[30] a) S. G. Hentges, K. B. Sharpless, *J. Org. Chem.* **1980**, *45*, 2257; b) H. Rubenstein, J. S. Svendsen, *Acta Chem. Scand.* **1994**, *48*, 439.

[31] This agreement between experiment and theory is remarkable, since DFT methods may slightly underestimate the strength of relatively weak metal–ligand bonds such as an Os–$NH_3$ bond in the presence of four very strong Os=O bonds; see, for example: a) D. V. Deubel, J. Sundermeyer, G. Frenking, *Inorg. Chem.* **2000**, *39*, 2314; b) D. V. Deubel, J. Sundermeyer, G. Frenking, *Org. Lett.* **2001**, *3*, 329; c) D. V. Deubel, J. Sundermeyer, G. Frenking, *Eur. J. Inorg. Chem.* **2001**, 1819.

[32] See: J. T. Anhaus, T. P. Kee, M. H. Schofield, R. R. Schrock, *J. Am. Chem. Soc.* **1990**, *112*, 1642.

[33] L. J. Goossen, H. Liu, K. R. Dress, K. B. Sharpless, *Angew. Chem.* **1999**, *111*, 1149; *Angew. Chem. Int. Ed.* **1999**, *38*, 1080.

[34] While the model cycles for catalytic diamination have been derived from state-of-the-art dihydroxylation and aminohydroxylation protocols, one may also consider additional sequences of reactions. Since hydrolysis is typically slower than cycloaddition and oxidation in dihydroxylation protocols, oxo–imido exchange may also occur prior to hydrolysis. Theory predicts reaction free enthalpies for the oxo–imido exchange of osma-2,5-diazolidines to be very similar to those of $OsO_4$ (12 kcal mol$^{-1}$) or $OsO_3$(NH) (13 kcal mol$^{-1}$), for example, 12 kcal mol$^{-1}$ for trioxoosma-2,5-diazolidine and 14 kcal mol$^{-1}$ for imidodioxoosma-2,5-diazolidine. If one wishes to consider ammoniolysis rather than hydrolysis and subsequent oxo–imido exchange, one may simply add the reaction free enthalpies of the latter two reactions.

[35] A. D. Becke, *J. Chem. Phys.* **1993**, *98*, 5648.

[36] Gaussian 98 (Revision A.7), M. J. Frisch, G. W. Trucks, H. B. Schlegel, G. E. Scuseria, M. A. Robb, J. R. Cheeseman, V. G. Zakrzewski, J. A. Montgomery, Jr., R. E. Stratmann, J. C. Burant, S. Dapprich, J. M. Millam, A. D. Daniels, K. N. Kudin, M. C. Strain, O. Farkas, J. Tomasi, V. Barone, M. Cossi, R. Cammi, B. Mennucci, C. Pomelli, C. Adamo, S. Clifford, J. Ochterski, G. A. Petersson, P. Y. Ayala, Q. Cui, K. Morokuma, D. K. Malick, A. D. Rabuck, K. Raghavachari, J. B. Foresman, J. Cioslowski, J. V. Ortiz, B. B. Stefanov, G. Liu, A. Liashenko, P. Piskorz, I. Komaromi, R. Gomperts, R. L. Martin, D. J. Fox, T. Keith, M. A. Al-Laham, C. Y. Peng, A. Nanayakkara, C. Gonzalez, M. Challacombe, P. M. W. Gill, B. G. Johnson, W. Chen, M. W. Wong, J. L. Andres, M. Head-Gordon, E. S. Replogle, J. A. Pople, Gaussian, Inc., Pittsburgh, PA, **1998**.

[37] P. J. Hay, W. R. Wadt, *J. Chem. Phys.* **1985**, *82*, 299.

[38] a) J. S. Binkley, J. A. Pople, W. J. Hehre, *J. Am. Chem. Soc.* **1980**, *102*, 939; b) W. J. Hehre, R. Ditchfield, J. A. Pople, *J. Chem. Phys.* **1972**, *56*, 2257.

[39] G. Frenking, I. Antes, M. Böhme, S. Dapprich, A. W. Ehlers, V. Jonas, A. Neuhaus, M. Otto, R. Stegmann, A. Veldkamp, S. F. Vyboishchikov, *Rev. Comput. Chem.* **1996**, *8*, 63.

[40] A. W. Ehlers, M. Böhme, S. Dapprich, A. Gobbi, A. Höllwarth, V. Jonas, K. F. Köhler, R. Stegmann, A. Veldkamp, G. Frenking, *Chem. Phys. Lett.* **1993**, *208*, 111.

[41] a) J. Cizek, *Adv. Chem. Phys.* **1969**, *14*, 35; b) G. D. Purvis, R. J. Bartlett, *J. Chem. Phys.* **1982**, *76*, 1910; c) G. E. Scuseria, C. L. Janssen,

  

H. F. Schaefer, III, *J. Chem. Phys.* **1988**, *89*, 7382; d) G. E. Scuseria, H. F. Schaefer, III, *J. Chem. Phys.* **1989**, *90*, 3700.
[42] J. A. Pople, M. Head-Gordon, K. Raghavachari, *J. Chem. Phys.* **1987**, *87*, 5968.
[43] A. E. Reed, L. A. Curtiss, F. Weinhold, *Chem. Rev.* **1988**, *88*, 899.
[44] A. D. Becke, *Phys. Rev. A* **1988**, *38*, 3098.
[45] C. Lee, W. Yang, R. G. Parr, *Phys. Rev. B* **1988**, *37*, 785.
[46] a) C. Fonseca Guerra, J. G. Snijders, G. Te Velde, E. J. Baerends, *Theor. Chem. Acc.* **1998**, *99*, 391; b) G. Te Velde, F. M. Bickelhaupt, E. J. Baerends, C. Fonseca Guerra, S. J. A. Van Gisbergen, J. G. Snijders, T. Ziegler, *J. Comput. Chem.* **2001**, *22*, 931.
[47] E. Van Lenthe, A. E. Ehlers, E. J. Baerends, *J. Chem. Phys.* **1999**, *110*, 8943, and references therein.
[48] J. G. Snijders, E. J. Baerends, P. Vernooijs, *At. Data Nucl. Data Tables* **1982**, *26*, 483.
[49] E. J. Baerends, D. E. Ellis, P. Ros, *Chem. Phys.* **1973**, *2*, 41.

Received: August 20, 2003 [F5467]

Published online: March 22, 2004